

EFFECTS OF AMINE AND ANHYDRIDE CURING AGENTS ON THE VARTM MATRIX PROCESSING PROPERTIES

Brian W. Grimsley[†], Pascal Hubert^{††}, Xiaolan Song^{†††},
Roberto J. Cano[†], Alfred C. Loos^{†††}, R. Byron Pipes^{††††}

[†] NASA Langley Research Center, Hampton, Virginia 23681

^{††} Old Dominion University, Norfolk, Virginia 23508

^{†††} Virginia Polytechnic Institute and State University, Blacksburg, Virginia 24061

^{††††} University of Akron, Akron, Ohio 44325

ABSTRACT

To ensure successful application of composite structure for aerospace vehicles, it is necessary to develop material systems that meet a variety of requirements. The industry has recently developed a number of low-viscosity epoxy resins to meet the processing requirements associated with vacuum assisted resin transfer molding (VARTM) of aerospace components. The curing kinetics and viscosity of two of these resins, an amine-cured epoxy system, Applied Poleramic, Inc. VR-56-4¹, and an anhydride-cured epoxy system, A.T.A.R.D. Laboratories SI-ZG-5A, have been characterized for application in the VARTM process. Simulations were carried out using the process model, COMPRO[®], to examine heat transfer, curing kinetics and viscosity for different panel thicknesses and cure cycles. Results of these simulations indicate that the two resins have significantly different curing behaviors and flow characteristics.

KEY WORDS: Epoxy, Composites, VARTM, Process Modeling

1.0 INTRODUCTION

The VARTM process has been developed over the last ten years for application in both commercial and military, ground-based and marine composite structures [1-3]. The process has advantages over conventional RTM because it eliminates the costs associated with matched-metal mold making and volatiles emission, while allowing low injection pressures [4].

In the VARTM process, the resin is injected through a single or multiple inlet ports depending upon part size and shape. A vacuum port allows the fiber preform to be evacuated prior to injection and provides the mechanism for transfer of the resin into the part. In addition to the

¹ Use of trade names or manufacturers does not constitute an official endorsement, either expressed or implied, by the National Aeronautics and Space Administration.

pressure gradient caused by the vacuum pressure, gravity and capillary flow effects must be considered [5]. The preform infiltration time is a function of the resin viscosity, the preform permeability and the applied pressure gradient. The infiltration time can be greatly reduced by utilizing a distribution medium with a higher permeability than the preform [6,7]. Consequently, the resin flows in the medium first and then the infiltration process continues through the preform thickness.

Recently, low viscosity VARTM epoxy resins have been developed by industry to meet the requirements for aerospace structure. As part of the NASA effort to further develop the VARTM process, several of these resins are being characterized and selected for use [8]. In addition to the required strength and durability of the polymer matrix, properties that govern the processing characteristics must be considered. A combination of experiments and process models have been used to characterize these resin systems and determine the influence of a larger number of polymer properties on final part quality. Further material development and characterization efforts can then be focused on the most important parameters for a given application.

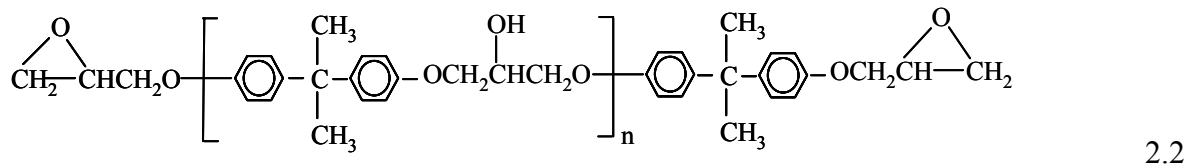
In the present work, the cure kinetics and viscosity of two chemically different VARTM epoxy resin systems are characterized. The resins selected for this work were SI-ZG-5A, a commercially available anhydride-cure epoxy blend VARTM resin developed at A.T.A.R.D Laboratories and an experimental amine-cure epoxy blend VARTM resin developed at Applied Poleramic, Inc. A process model was used to study and compare the resin curing behavior for different process cycles and panel thicknesses.

2.0 BACKGROUND

The crosslinked polymer epoxy is derived from reactions of the epoxy group, or epoxide, shown in Equation 2.1 below.



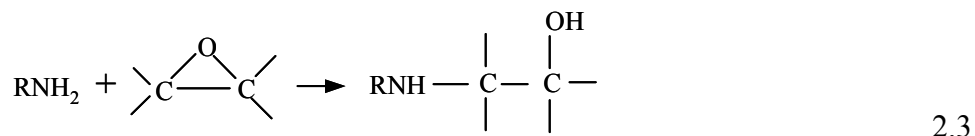
Most commercial epoxy resins are synthesized from the reaction of two or more moles of epichlorhydrin and one mole of bisphenol A [9]. This results in the uncrosslinked resin diglycidyl ether of bisphenol A (DGEBA) shown in Equation 2.2 with the epoxide group at each end. With n=1, this is the most basic form of liquid epoxy resin.



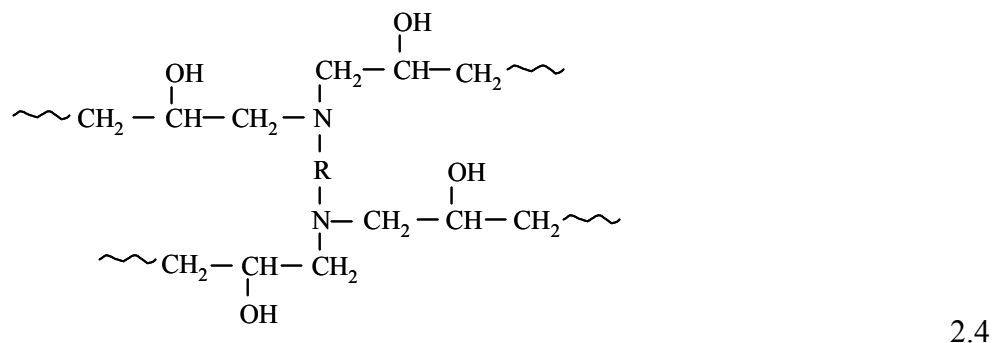
The functionality and reactivity of the epoxy resin molecule is, in part, dictated by the epichlorhydrin monomer, which can have two or more epoxide groups at varying locations depending on its prior reaction with a variety of hydroxy, carboxy and amino compounds.

The resulting epoxy resin can then be reacted with a curing agent to form a solid crosslinked epoxy network. Several basic types may be chosen according to factors such as the steric nature and functionality of the epoxy resin as well as the desired mechanical and thermal properties of the cured epoxy [10]. Of interest here are the amine and anhydride type curing agents.

Aromatic primary amines such as m-Phenylenediamine (m-PDA) require the presence of a hydrogen donor compound such as a hydroxyl group (benzene, acetone, water) in order to react with the epoxy ring. Equation 2.3 shows the addition-reaction of a primary amine (RNH₂) with the epoxy ring, where, for m-PDA, R = H₂NC₆H₄.

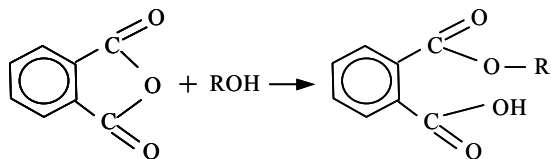


When this occurs, the initial reaction product is a hydroxyl and a secondary amine (RNH). The secondary amine and the hydroxyl can then open the epoxy ring of another DGEBA molecule creating a crosslink between the two as shown in Equation 2.4, where R=C₆H₄. This reaction continues throughout the bulk of the epoxy resin/curing agent mixture with the primary amines usually reacting twice as quickly with the DGEBA molecules as the secondary amines react [9].



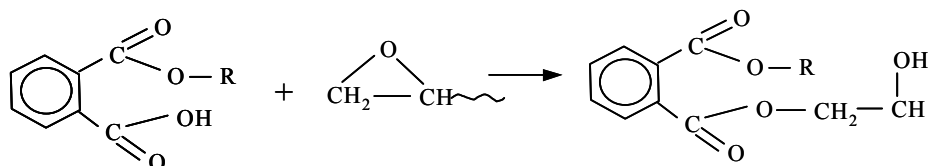
This reaction results in a tertiary amine. The resulting tertiary amine in this case usually lacks the reactivity to continue catalytic activity. Some secondary aromatic amines such as diethanolamine and also tertiary amines such as dimethylethanolamine and diethylethanolamine can be introduced to the epoxy resin to act as the sole curing agent [9]. The tertiary amine is an organic base containing an atom with an unpaired electron in its outer orbital. In this case, the tertiary amine approaches one of the carbon atoms of the epoxide group and, in the presence of a hydroxyl group, bonds to the oxygen atom of the epoxy. From this an anion is generated, which is capable of opening a second epoxy ring and, thus continues the crosslink reaction.

The other epoxy system investigated uses anhydride curing agents. Cyclic anhydrides, such as the aromatic phthalic anhydride (PA), will not react directly with the epoxide group. The anhydride ring must first be opened by active hydrogen present as water, hydroxyls, or a Lewis base. The addition of a hydroxyl group to the PA compound, shown in Equation 2.5 with R= ~CH₂-CH-CH₂~, results in the organic acid carboxyl group which can then react with the DGEBA molecule.



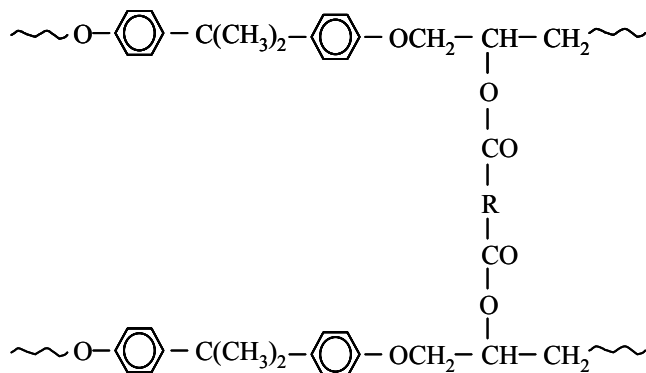
2.5

The crosslinking epoxy reaction is quite complex involving addition esterification with the formed carboxyl group and/or by condensation reactions of pendant hydroxyl groups [9]. The un-catalyzed epoxy-carboxyl reaction shown in Equation 2.6 will occur slowly without the presence of proton donors [11].



2.6

The final crosslinked, phthalic anhydride-cured epoxy is shown in simplified form in Equation 2.7, where $R=C_6H_4$.



2.7

Some generalizations have been made in the literature regarding the comparison of amine-cured versus anhydride-cured epoxies [9] and [11]. The amines are more toxic causing skin and respiratory irritation, however, this can be alleviated if the amines are used in the form of adducts. The stoichiometric ratio of the epoxy/amine reaction requires careful measurement of the epoxy resin and curing agent. The aromatic amines offer superior resistance to chemical attack. Anhydrides reportedly give lower exotherms during cure and generally provide better thermal stability and electrical insulation. The majority of anhydride-cured epoxies are more brittle than the amine-cured. Toughening with flexibilizers generally results in lowered heat resistance.

Both the amine-cured epoxy VR-56 and the anhydride-cured epoxy SI-ZG-5A are proprietary blends of several different epoxy resins and several different amine and anhydride curing agents, respectively. The epoxy resins present in these blends may have different functionalities and reactivities and the curing agents may be present in liquid eutectics and adducts. Cure kinetics characterization can be difficult due to the complex and proprietary nature of these blended resins. In addition, the generalizations found in the literature may or may not be relevant.

3.0 MATRIX CHARACTERIZATION

Accurate prediction of many of the key material properties required in composites process models such as resin viscosity, modulus development and cure shrinkage depend on an accurate knowledge of the cure state of the resin during processing. Furthermore, an understanding of resin viscosity behavior is also required to predict the flow of resin during VARTM infiltration. Cure kinetics and viscosity models are obtained for the resin using a combination of isothermal and dynamic differential scanning calorimeter (DSC) and parallel-plate rheometer scans, respectively.

3.1 Cure kinetics model All tests were performed on a Shimadzu DSC-50 differential scanning calorimeter. The total heat of reaction (H_R) was measured from dynamic scans at 1.1°C/minute from room temperature up to 250°C. The isothermal tests were performed at temperatures ranging from 60°C to 140°C. In these tests, the specimens were dropped into a DSC cell that had been heated to the desired temperature. The specimens were maintained and scanned at these temperatures for up to 12 hours, and then rapidly cooled. The isothermal tests were followed by a dynamic scan at 1.1°C/minute to measure the residual heat of reaction.

Raw data from the DSC experiments consisted of measurements of heat flow and total resin heat of reaction as calculated by the apparatus software. From the heat flow curves obtained from the dynamic runs (Figure 1), H_R for the anhydride-cured SI-ZG-5A and the amine-cured VR-56-4 were determined to be almost identical: 350 kJ/kg and 353 kJ/kg, respectively. However, the peak shape and location for each resin system was different. The peak for SI-ZG-5A occurred at a lower temperature (112°C) compared to VR-56-4 (120°C). Furthermore, the width of the exothermic peak was narrower for SI-ZG-5A indicating that the reaction rate was higher compared to VR-56-4. From the baseline heat flow ($\dot{q}_{baseline}$) and the total heat flow, the resin cure rate was then determined for each epoxy using:

$$\frac{d\alpha}{dt} = \frac{(\dot{q}_{baseline} - \dot{q}_{in}) / m_{sample}}{H_R / (1 - \alpha_0)} \quad 3.1$$

where, \dot{q}_{in} is the measured heat flow, m_{sample} is the sample mass and α_0 is the starting resin degree of cure, assumed to be 0.01 in all cases. Resin degree of cure as a function of time was determined by integrating the calculated cure rate. From Figure 2, two distinct peaks in the VR-56-4 isothermal curve can be observed. These two peaks were present to some degree in all of the isothermal scans for this resin.

For SI-ZG-5A, the equation chosen for the cure kinetics model is a modified auto-catalytic equation, modified to account for a shift from kinetics to diffusion control [8].

$$\frac{d\alpha}{dt} = \frac{K\alpha^m(1-\alpha)^n}{1 + e^{C\{\alpha - (\alpha_{c0} + \alpha_{cr}T)\}}} \quad 3.2$$

$$K = Ae^{(-\Delta E/RT)}$$

The parameters used to fit this model to the experimental data were developed in a previous study [8]. In this present work, the parameters were updated to account for long isothermal holds up to twelve hours.

The cure kinetics for the VR-56-4 was more complex. The two peaks in the isothermal heat flow curve shown in Figure 2 reveals two separate reactions occurring during cure. It was determined that the first reaction for $\alpha < 0.10$ which probably corresponds to the primary amine reaction discussed in Section 2. Therefore, an n^{th} -order rate equation (Equation 3.3) was used to calculate $d\alpha/dt$ for $\alpha < 0.10$. For $\alpha \geq 0.10$, the modified, auto-catalytic equation (Equation 3.2) is used to calculate $d\alpha/dt$.

$$\begin{aligned} \frac{d\alpha}{dt} &= A_2 e^{(-\Delta E_2 / RT)} (1 - \alpha)^{n_2} & \alpha < 0.1 \\ \frac{d\alpha}{dt} &= \frac{K\alpha^m (1 - \alpha)^n}{1 + e^{C\{\alpha - (\alpha_{c0} + \alpha_{CT}T)\}}} & \alpha \geq 0.1 \\ K &= Ae^{(-\Delta E / RT)} \end{aligned} \quad 3.3$$

The significance of the various terms in Equations 3.2 and 3.3 is presented in Table 1. The activation energies, ΔE and ΔE_2 , were calculated from the slope of the natural logarithm of the isothermal cure rate, $\ln(d\alpha/dt)$, vs. $1/T$ at a number of different resin degrees of cure. All other model constants were determined using a weighted least-squares analysis, using data from both isothermal and dynamic DSC measurements.

Table 1 Parameters used in SI-ZG-5A and VR-56-4 kinetics model (Equations 3.2 and 3.3).

Parameter	Value	
	SI-ZG-5A	VR-56-4
Activation energy	$\Delta E = 61.0$ kJ/gmole	$\Delta E = 48.8$ kJ/gmole
Pre-exponential cure rate coefficient	$A = 4.11 \times 10^5$ /s	$A = 2.46 \times 10^3$ /s
First exponential constant	$m = 0.551$	$m = 0.475$
Second exponential constant	$n = 1.00$	$n = 1.09$
Diffusion constant	$C = 40$	$C = 10$
Critical degree of cure at $T = 0^\circ\text{K}$.	$\alpha_{c0} = 0.216$	$\alpha_{c0} = 0.748$
Constant accounting for increase in critical resin degree of cure with temperature	$\alpha_{CT} = 1.3 \times 10^{-3}/\text{K}$	$\alpha_{CT} = 5.7 \times 10^{-4}/\text{K}$
Activation energy for initial reaction	-	$\Delta E_2 = 47.2$ kJ/gmole
Pre-exponential cure rate coefficient (initial reaction)	-	$A_2 = 1.13 \times 10^3$ /s
Exponential constant (initial reaction)	-	$n_2 = 1.09$

Figure 3 compares the model predictions for the rate of cure versus degree of cure for the 100°C isothermal hold. The modified catalytic equation is shown to work very well in both cases. For

VR-56-4, the initial reaction occurring at $\alpha < 0.10$ is also well captured. Figures 4 and 5 show that the models provide an excellent fit to the isothermal cure tests at all temperatures examined. In Figure 4, for VR-56-4 the only discrepancy is found at $\alpha > 0.8$ for the 120°C and 140°C case. In Figure 5, the only discrepancy between the model and the experiments is found for times greater than twelve hours in the 60°C case.

3.2 Viscosity model A Rheometric Ares System-Five parallel-plate rheometer was used to measure the neat resin viscosity. The viscosity model constants for both resins were determined by a series of isothermal cure tests ranging from 60°C to 140°C. Dynamic cures at 1.1°C/minute and a typical cure cycle test were conducted to validate the models. The samples were sheared between two 30 mm parallel discs. A dynamic or sinusoidal wave torque signal was applied to the sample. The frequency of the signal was 100 rad/s at a maximum shear strain of 10%. The test was stopped when the resin reached its gel point or after twelve hours, whichever came first. The room temperature viscosity for SI-ZG-5A and the VR-56-4 were measured at 0.32 Pa·s and 0.42 Pa·s, respectively.

The viscosity model [8] used in this study is as follows:

$$\mu = A_{\mu} \exp(E_{\mu} / RT) [\alpha_g / (\alpha_g - \alpha)]^{(A+B\alpha)} \quad 3.4$$

where A_{μ} , E_{μ} , A and B are experimentally determined parameters, R is the universal gas constant and α_g is the degree of cure at gelation. The slope of a linear regression through the data of $\ln\mu$ versus $1/T$ at low resin degree of cure ($\alpha \approx 0$) yields the values for E_{μ} . The data from the dynamic runs at 1.1°C/minute results was used in this calculation for both resins. The gel point degree of cure (α_g) was evaluated from the crossover point between the storage and the loss modulus (G' and G''). The gel point was 0.60 for SI-ZG-5A and 0.86 for VR-56-4. To evaluate the other constants, a best fit was done by changing the constants A_{μ} , A and B to fit the experimental data from the isothermal and dynamic tests. The best-fit constants are given in Table 2.

Table 2 Parameters used in SI-ZG-5A and VR-56-4 viscosity model (Equation 3.4).

Parameter	Value	
	SI-ZG-5A	VR-56-4
Activation energy	$E_{\mu} = 54803$ J/gmole	$E_{\mu} = 56000$ J/gmole
Pre-exponential coefficient	$A_{\mu} = 8.3 \times 10^{-11}$ Pa·s	$A_{\mu} = 6.5 \times 10^{-11}$ Pa·s
First exponential constant	$A = 4$	$A = 4.23$
Second exponential constant	$B = 6.25$	$B = 0$
Degree of cure at gel point	$\alpha_g = 0.60$	$\alpha_g = 0.86$

Figure 6 shows the comparison of the model prediction to the experimental data in a typical cure temperature cycle test for SI-ZG-5A and VR-56-4. In both cases, the models capture the ambient viscosity, the reduction in viscosity due to temperature increase, and the rapid increase in viscosity as the resins reach the gel point. Furthermore, for the temperature cycle shown, the

VR-56-4 epoxy is found to have a more gradual increase in viscosity during the 66°C hold. This resin must be heated to a higher temperature in order to reach gelation.

4.0 CURE SIMULATIONS

The difference in curing behavior between VR-56-4 and SI-ZG-5A for typical VARTM panels was investigated using the process model COMPRO[®] [12]. Cure simulations of 5 mm and 25 mm thick panels were performed. The preform characteristics used in the simulations were from the SAERTEX [13] multi-axial, non-crimp carbon fiber fabric with a stacking sequence of [-45,45,0,90,0,45,-45]_n. Two different cure cycles with specifications summarized in Table 3 were considered. Cycle 1 is the resin manufacturer recommended cycle for SI-ZG-5A, cycle 2 is a composites manufacturer suggested cure cycle. The cure kinetics and viscosity model developed in this work for SI-ZG-5A and VR-56-4 were used in the simulations. The panel was assumed to be fully saturated with resin at a fiber volume fraction of 0.50. Thermal properties for the resin and the fiber were taken for a typical epoxy and carbon fiber. The panel, the 3 mm thick steel tool and the distribution media were modeled with a one-dimensional column of elements in the thickness direction. The Plastinet[®] distribution media was modeled as a nylon/resin composite with a fiber volume fraction of 0.23 and a thickness of 2 and 3 mm for the 5 mm and 25 mm panel respectively. A convective heat transfer boundary condition (20 W/m²°C heat transfer coefficient) was assumed on the top and bottom of the tool-part assembly. The heat transfer and resin cure kinetics were solved and resin flow during cure was neglected.

Table 3 summarizes the results of the simulations and Figures 7, 8, 9 & 10 present the maximum part temperature and minimum resin viscosity profiles predicted by the model. It is clear that the two resin systems have significantly different curing behaviors. SI-ZG-5A has a faster gel time (an average of 162 min more quickly) than VR-56-4, but has a higher exothermic temperature for the 25 mm panel (up to +31°C). Both systems have similar minimum viscosity. VR-56-4 cure is more sensitive to the cure cycle selected in this study as using cycle 2 reduces the exothermic temperature by 14°C and increases the gel time by 132 minutes. This difference between cycle 1 and 2 is not observed for SI-ZG-5A. VR-56-4 cure is more gradual and occurs at higher temperature and the results of the simulation clearly illustrate that behavior. The flow number (FN) presented in Table 1 gives an indication on the amount of flow possible before gelation and was calculated using the following relation:

$$FN = \int_0^{t_{gel}} 1/\mu(t) dt \quad 4.5$$

From Table 3, the flow number for VR-56-4 is about twice the value for SI-ZG-5A, which indicates that more resin flow before gelation could occur with VR-56-4. This analysis stresses the importance of understanding the curing behavior of the resin systems considered for a particular application and the relationship between part geometry and curing conditions. The use of a process model like COMPRO provides a framework for the development and understanding of the curing strategies for components manufactured by the VARTM process.

Table 3 Results from the cure simulations.

Case	Exotherm Temperature (°C)	Minimum Viscosity (Pa.s)	Gel Time (min)	Flow Number (s/(Pa.s))
SAERTEX/SI-ZG-5A				
5 mm panel, Cycle 1*	4	0.031	191	128577
5 mm panel, Cycle 2**	4	0.034	212	130610
25 mm panel, Cycle 1	42	0.036	161	128831
25 mm panel, Cycle 2	42	0.037	182	130561
SAERTEX/VR-56-4				
5 mm panel, Cycle 1	7	0.033	290	280302
5 mm panel, Cycle 2	2	0.034	412	273814
25 mm panel, Cycle 1	25	0.034	280	281309
25 mm panel, Cycle 2	11	0.035	412	277117

* Cycle 1: Ramp to 66°C @ 1.11°C/min, Hold 2.75 hours, Ramp to 121°C @ 0.83°C/min, Hold 2.5 hours, Ramp to 177°C @ 0.56°C/min, Hold 6 hours, Ramp to RT @ -0.56°C/min.

** Cycle 2: Ramp to 66°C @ 0.56°C/min, Hold 4 hours, Ramp to 177°C @ 0.56°C/min, Hold 6 hours, Ramp to RT @ -0.56°C/min.

5.0 SUMMARY

The properties that govern the processing characteristics have been characterized for an amine-cured, VR-56-4, and an anhydride-cured, SI-ZG-5A, epoxy system. Relationships for resin viscosity and degree of cure were shown to accurately model the observed resin characteristics. Results of cure simulations performed using a process model show that the two resins have similar minimum viscosities but significantly different curing behaviors. The cure reaction of SI-ZG-5A occurs more quickly and at a lower temperature, but with a higher exotherm than that of the VR-56-4 resin. Both curing cycles examined show that time to resin gel and exotherm are strong functions of the cure cycle characteristics and resin properties. However, the VR-56-4 appears to be more sensitive to the cure cycle selection. Despite its higher initial viscosity, the calculated flow number, an indication of potential resin flow, for the VR-56-4 is about twice as large as that found for SI-ZG-5A.

6.0 REFERENCES

- [1] S. M. Lewit and J.C. Jakubowski, 1997. "Low Cost VARTM Process for Commercial and Military Applications", SAMPE International Symposium, 42, 1173.
- [2] L.B. Nquyen, T. Juska and S. J. Mayes, 1997. "Evaluation of Low Cost Manufacturing Technologies for Large Scale Composite Ship Structures", AIAA/ASME/ASCE/AHS/ASC Structures, Structural Dynamics, and Materials Conference, 38, 992.
- [3] P. Lazarus, 1996. "Resin Infusion of Marine Composites", SAMPE International Symposium, 41, 1447.

- [4] J. R Sayre, 2000. "RFI and SCRIMP Model Development and Verification", Ph.D. Dissertation, Department of Engineering Science and Mechanics, Virginia Polytechnic Institute and State University, Blacksburg, VA.
- [5] A.C. Loos, J. Sayre, R. McGrane and B. Grimsley, 2001. "VARTM Process Model Development", SAMPE International Symposium, 46, 1049.
- [6] Seemann, W.H., 1990. U.S. Patent 4,902,215.
- [7] Seemann, W.H., 1994. U.S. Patent 5,316,462.
- [8] B.W. Grimsley, P.Hubert, T.H.Hou, R.J.Cano, A.C.Loos, R.B.Pipes, "Matrix Characterization and Development for the Vacuum Assisted Resin Transfer Molding Process", ASC Technical Conference, 16, CD.
- [9] H. Lee and K. Neville, Handbook of Epoxy Resins, McGraw-Hill Book Company, New York, 1967, pp. 5.2-5.13.
- [10] George Odian, Principles of Polymerization, John Wiley and Sons, New York, 1991, pp. 134.
- [11] K.J. Saunders, Organic Polymer Chemistry, Chapman and Hall, London, 1988, pp. 424-427.
- [12] G. Fernlund, A. Poursartip, K. Nelson, M. Wilenski and F. Swanstrom, 1999. "Process Modeling for Dimensional Control – Sensibility Analysis of a Composite Spar Process", SAMPE International Symposium, 44, 1744.
- [13] SAERTEX[®], Wagener GmbH & Co. KG, 48369 Saerbeck, Germany.

7.0 FIGURES

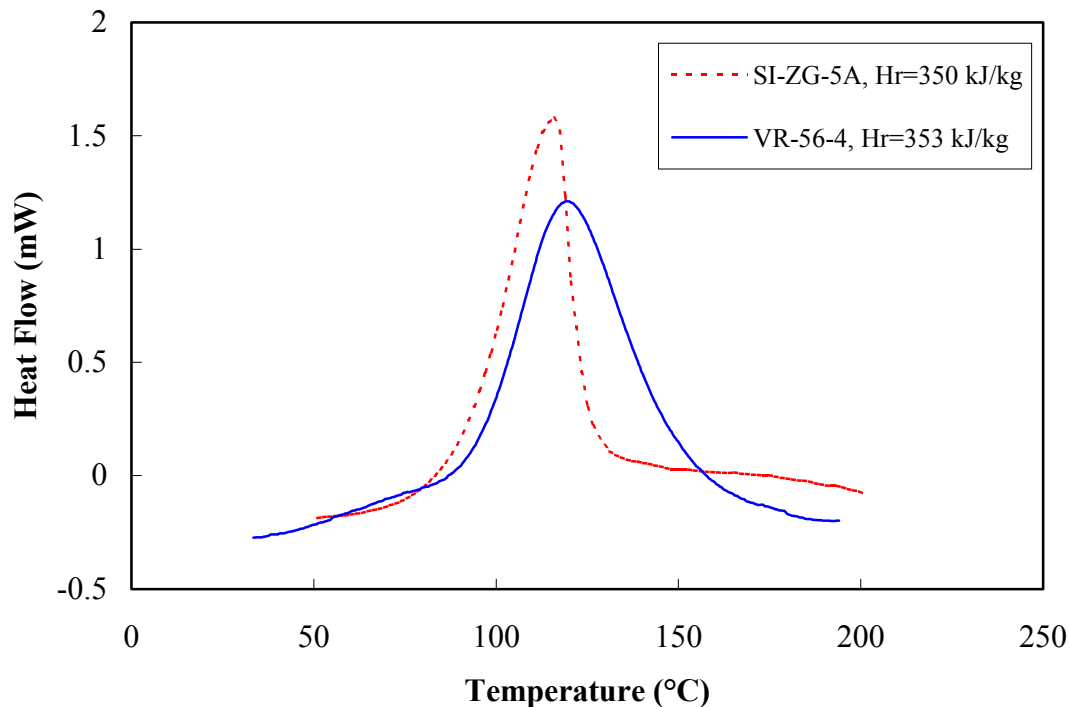


Figure 1 Typical dynamic scans for SI-ZG-5A and VR-56-4 at 1.1 °C/min, showing the total heat of reaction.

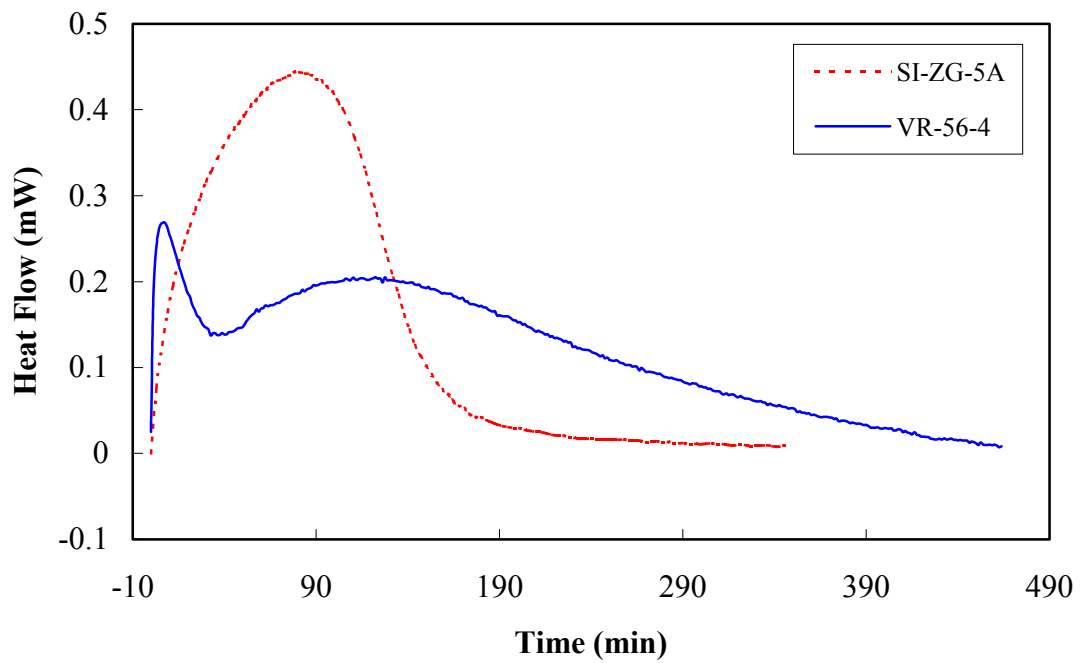


Figure 2 Isothermal scans of SI-ZG-5A and VR-56-4 at 80°C for 6hrs and 8hrs, respectively.

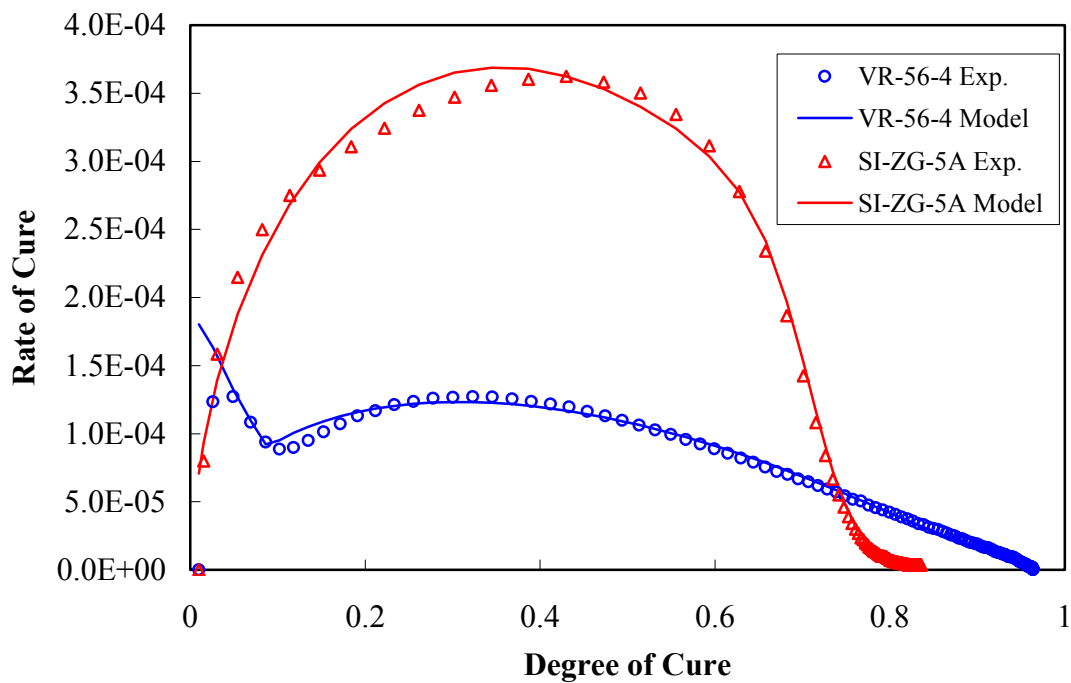


Figure 3 Calculated model fits to experimental data for SI-ZG-5A and VR-56-4 at 100°C isothermal cure.

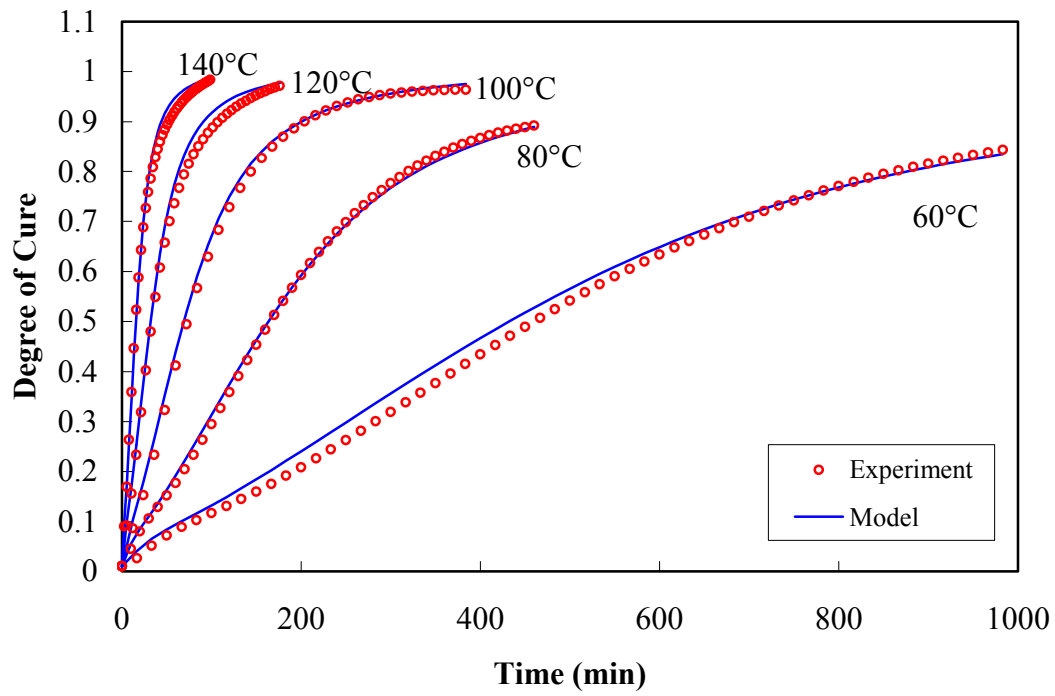


Figure 4 Comparison between measured and predicted VR-56-4 resin degree of cure in isothermal curing condition.

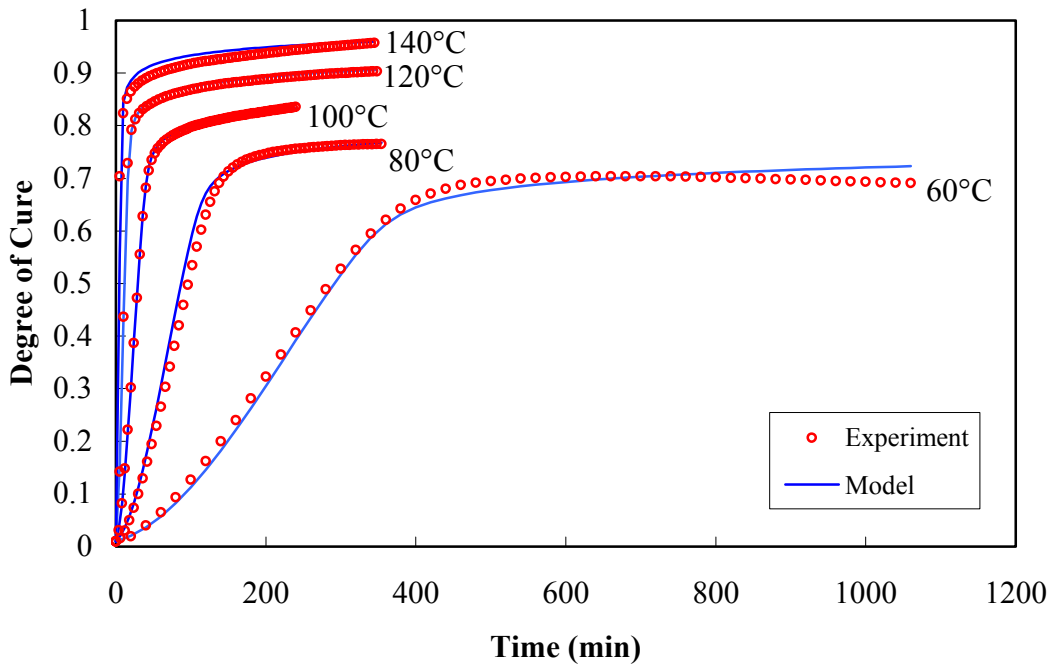


Figure 5 Comparison between measured and predicted SI-ZG-5A resin degree of cure in isothermal curing condition.

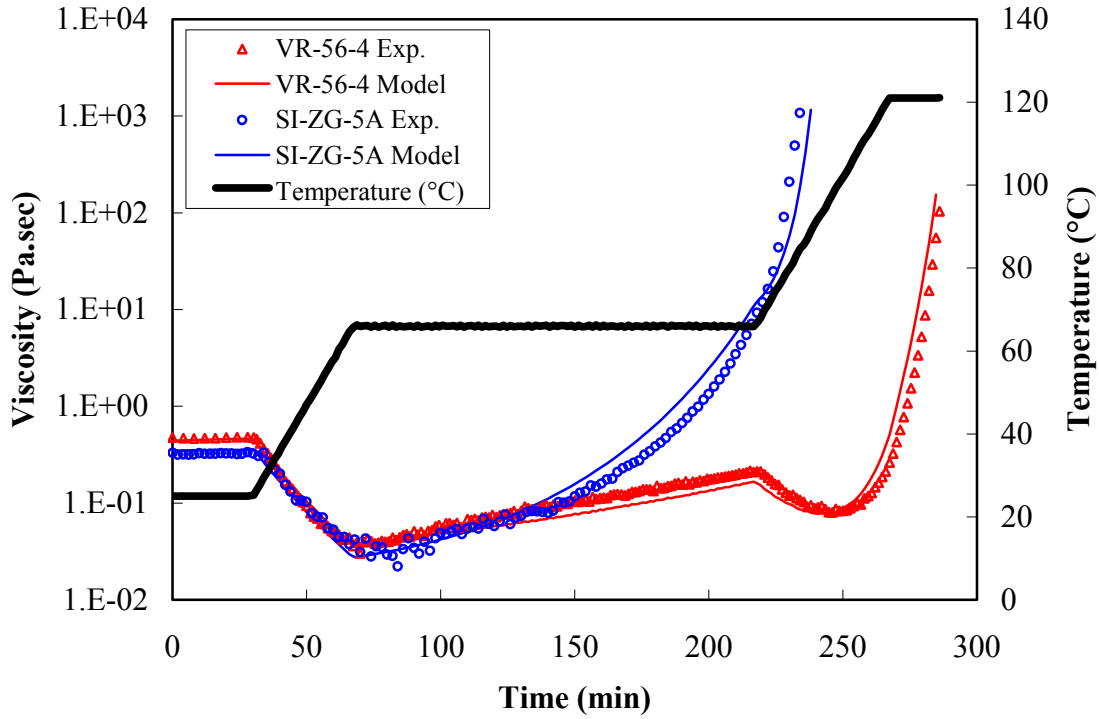


Figure 6 Comparison between measured and predicted viscosity for a typical cure cycle test for SI-ZG-5A and VR-56-4.

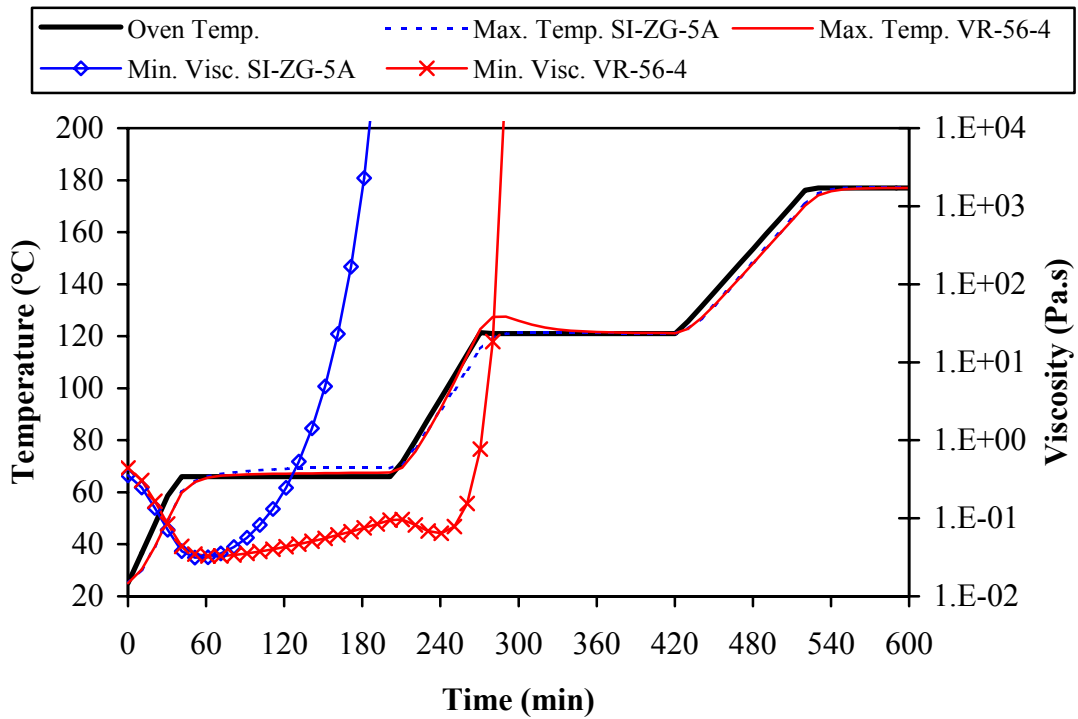


Figure 7 Predicted maximum part temperature and minimum resin viscosity for a 5mm thick SAERTEX fabric panel cured following cycle 1 (SAERTEX/SI-ZG-5A and SAERTEX/VR-56-4).

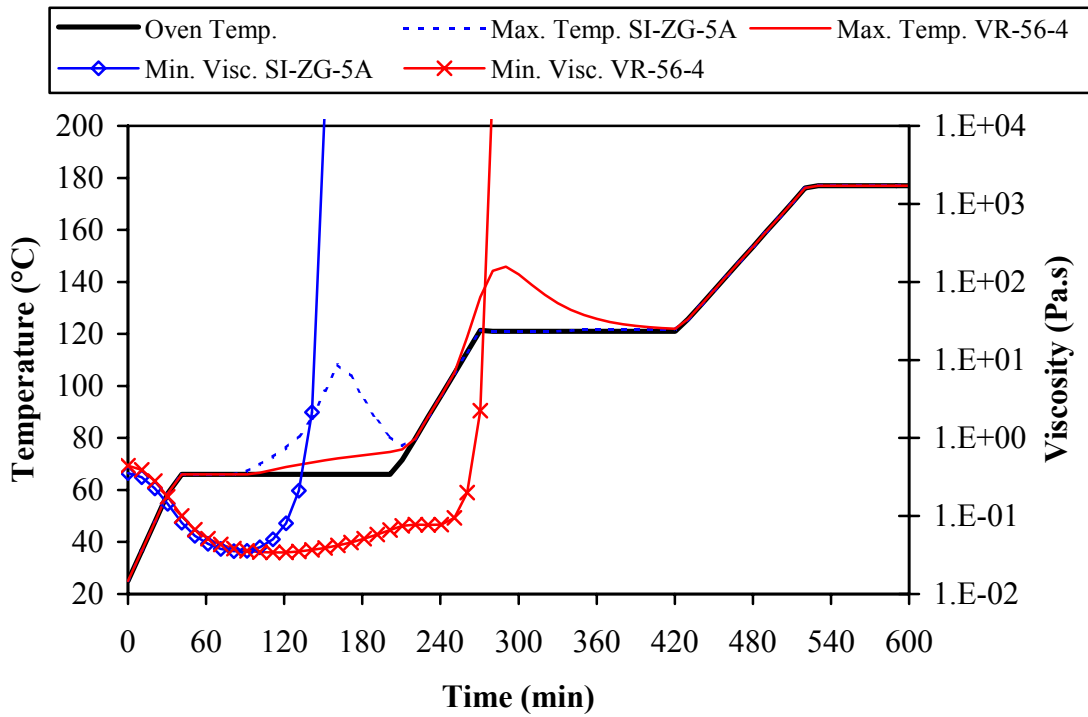


Figure 8 Predicted maximum part temperature and minimum resin viscosity for a 25mm thick SAERTEX fabric panel cured following cycle 1 (SAERTEX/SI-ZG-5A and SAERTEX/VR-56-4).

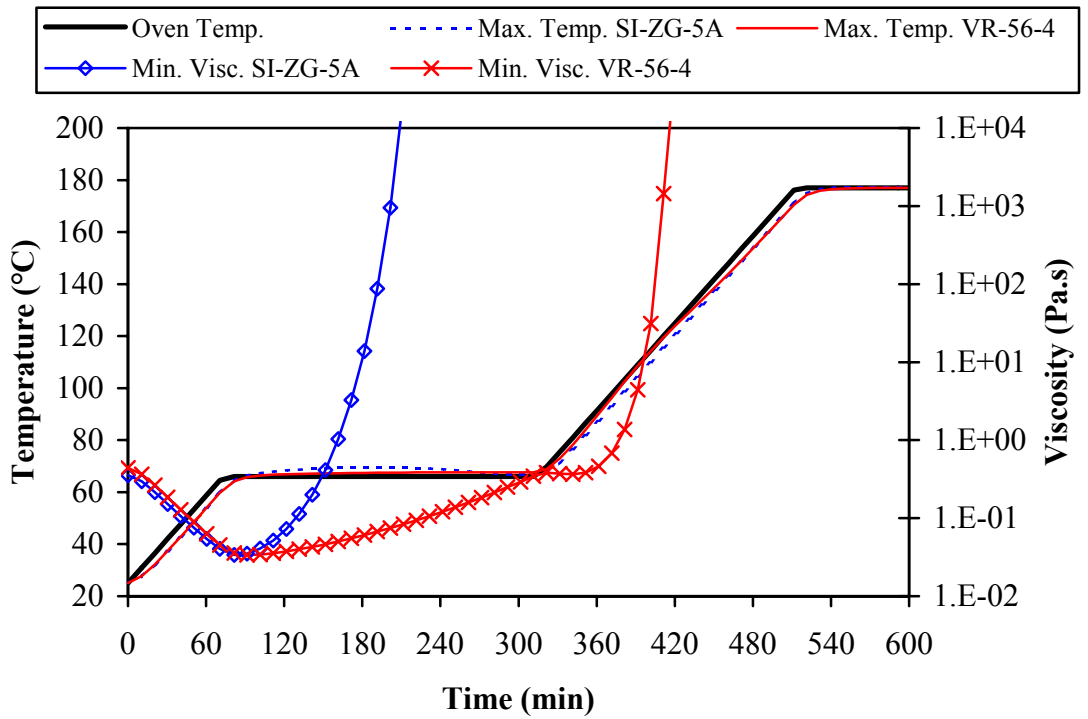


Figure 9 Predicted maximum part temperature and minimum resin viscosity for a 5mm thick SAERTEX fabric panel cured following cycle 2 (SAERTEX/SI-ZG-5A and SAERTEX/VR-56-4).

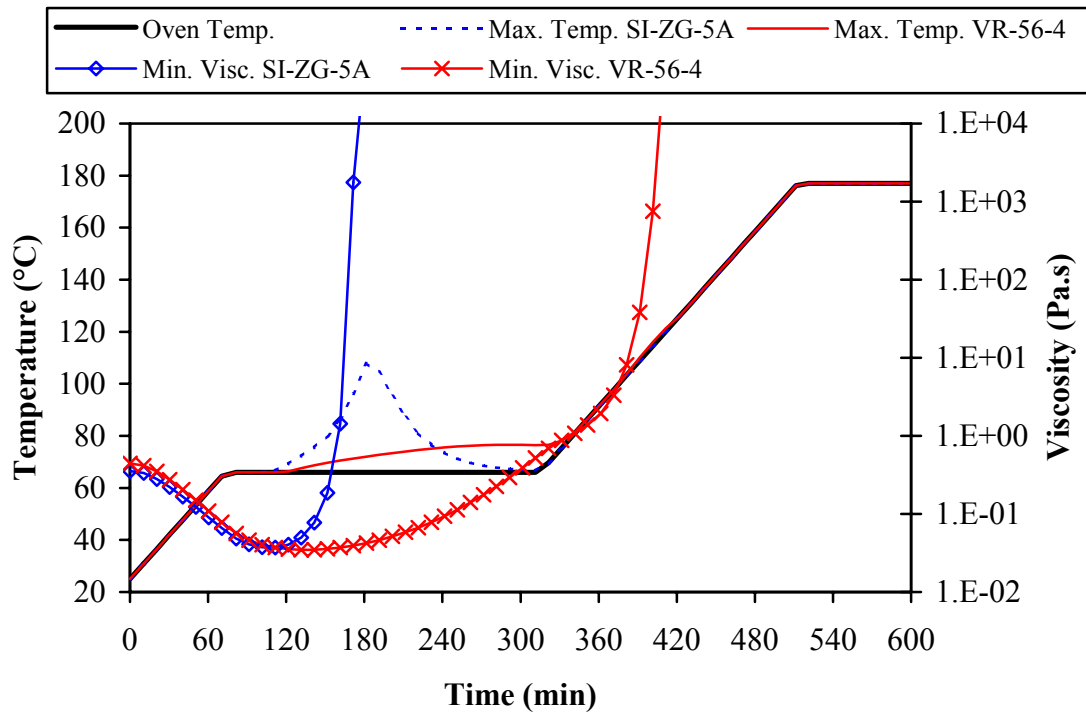


Figure 10 Predicted part maximum part temperature and minimum resin viscosity for a 25mm thick SAERTEX fabric panel cured following cycle 2 (SAERTEX/SI-ZG-5A and SAERTEX/VR-56-4).